Journal of Heat and Mass Transfer Research

Journal homepage: http://jhmtr.semnan.ac.ir

Semnan University

Numerical Simulation of Combined Transient Natural Convection and Volumetric Radiation inside Hollow Bricks

Mohammad Omidpanah[a], Seyed Ali Agha Mirjalily [*,b], Hadi Kargarsharifabad[c], Shahin shoeibi[c]

[a]*Department of Mechanical Engineering, Faculty of Shahid Sadooghi, Yazd Branch, Technical and Vocational University (TVU), Yazd, Iran.*
[b]*Department of Mechanical Engineering, Yazd Branch, Islamic Azad University, Yazd, Iran.*
[c]*Energy and Sustainable Development Research Center, Semnan Branch, Islamic Azad University, Semnan, Iran.*

PAPER INFO

Paper history:
Received: 2020-09-14
Revised: 2021-07-10
Accepted: 2021-07-17

Keywords:
radiation;
conjugate heat transfer;
transient;
discrete ordinate method.

ABSTRACT

This study simulated the flow and temperature field inside hollow bricks using well-known geometries to investigate the transient thermal behavior in both solid and fluid regions. To this end, a set of governing equations was solved simultaneously for an absorbing-emitting, isotropically scattering gas and solid region. To discretize the equations, the finite volume method was applied and the radiative transfer equation was calculated using the discrete ordinate method. Furthermore, the block off method is used to distinguish between solid and fluid media in the computational domain. The obtained results show that the rate of heat transfer is minimized in geometries having vertical rectangle sub cavities and their wall emissivity tends to zero. Moreover, the time required to reach steady state condition is an increasing function of total heat flux.

DOI: 10.22075/JHMTR.2021.21371.1306

1. Introduction

Here introduces the paper, As an undeniable fact, burning of fossil fuels leads to global warming and climate change. This is leads to consumption of more energy for air conditioning of buildings, especially in the Middle East. To meet this challenge, hollow bricks can be applied in building structures to save energy. In this regard, the optimum geometry for minimum heat transfer should be determined. To hit this target, a detailed simulation was implemented, including all aspects of heat transfer, such as conduction, natural convection, and volumetric radiation.

Regarding the investigation of heat transfer in cavities, Moufekkir et al. [1] numerically investigated combined natural convection and volumetric radiation in a cavity containing a homogeneous, gray, absorbing, emitting, and isotropic scattering media. The right and left boundaries of the cavity were isotropic at T_h and T_c, respectively. Furthermore, the cavity was perfectly insulated on the walls, top, and bottom. Volumetric radiation plays a significant role in velocity and temperature fields, so that the absence of this mechanism can make asymmetric changes in distributions of temperature and flow fields. Vivek et al. [2] analyzed the interaction effects between surface radiation and natural convection in an air-filled tilted enclosure. They obtained the maximum convective and radiative Nusselt numbers for the angle of tilt as $\theta = +15$ and $\theta = -15$, respectively. Moreover, surface radiation has a remarkable effect on temperature and velocity fields. Zhang et al. [3] study conjugate conduction of natural convection in a cavity with conducting walls. They investigated the effects of inclination angle on the Nusselt number in the absence of radiation heat transfer in a condition that the temperature imposed on the hot wall was periodic and depended on time. Foruzan Nia et al. [4] study combined natural convection and volumetric radiation in a cavity equally partitioned by conducting walls. Each division was filled with gases of different optical thickness as well as absorbing and emitting capability. According to the obtained results, when the optical thickness of the gas layer in the left enclosure is greater than the right one, the field reaches its minimum

[*]*Corresponding Author: Seyed Ali Agha Mirjalily, Department of Mechanical Engineering, Yazd Branch, Islamic Azad University, Yazd, Iran.*
Email: SAA_mirjalily@iauyazd.ac.ir

temperatures. Martyushev et al. [5] conducted a three-dimensional investigation over conjugate natural convection and surface radiation in a cubic cavity with conducting walls. Their findings showed a correlation between the results of 2-D and 3-D models. As they concluded, the average convection Nusselt is an increasing function of Rayleigh number.

Regarding the investigation of hollow bricks in terms of heat transfer, Al-Hazmy [6] numerically simulated three configurations of hollow bricks. These bricks typically contain three hollow cells, made of polystyrene bars and filled with polystyrene. Results showed that the insertion of polystyrene bars significantly decreased the heat rate by 36%. However, the effects of radiation heat transfer were neglected in this study. Young and Vafai [7] first simulated flow and heat transfer in a horizontal channel containing a large array of heated obstacles. Kim et al. [8] studied the thermal behavior of heated electronic components in pulsating channel flow. Bhomik et al. [9] investigated the effect of flow rates and geometrical parameters on convective cooling of discrete heat sources in a rectangular channel. The channel is assumed to be cooled with liquid. The results indicate that the Reynolds number intensely affects the heat transfer coefficient and fully-developed values for this coefficient are achieved before the first component. Hamouche and Bessaih [10] applied the SIMPLER algorithm to numerically simulate mixed convection air cooling of two identical protruding heat sources inside a two-dimensional horizontal channel. The authors found an heat transfer inside the channel is improved by increasing the separation distance of electronic chips. Mixed convection cooling of a transverse fin in an inclined parallel channel was numerically studied by Yang et al. [11]. Boutina and Bessaih [12] analyzed mixed convection cooling of electronic chips inside an inclined channel for 5 values of inclination angle. The results show the maximum heat transfer rate is obtained for Ɵ=45.

Nowadays, researchers prefer to analyze the heat transfer between solid and fluid domains by exchanging thermal energy at the interfaces between them, which is known as conjugate heat transfer. Mathews and Balaji [13] numerically simulated conjugate heat transfer inside a vertical channel with discrete heat sources. The researchers show to reduce the maximum temperature of the electronic components, the thermal conductivity of printed circuit boards (PCB) should be increased. Premachandran and Balaji [14] studied the conjugate mixed convection with surface radiation from horizontal channels containing protruding heat sources. Investigation of conjugate heat transfer and the second law analysis in a two-dimensional rectangular channel with wall-mounted heat sources was studied recently [15,16]. Recently, Datta et al. [17] conjugate heat transfer under study inside a three-dimensional rectangular microchannel with trapezoidal cavities and ribs. The transient analysis of forced convection in channels has been an interesting subject for scientists [18, 19]. Lately, Knupp et al. [20] applied generalized integral transform technique to numerically investigate transient behavior of conjugate heat transfer in laminar microchannel flow.

In all of the previous works mentioned, the effect of radiation heat transfer was neglected for simulation of heat removal from the components. The radiation effect on flow is most significant when flowing substance treats as participating media. Energy transfer and thermal analysis of the combined mode of radiation and convection heat transfer have been studied by researchers during past years [21–24]. Ansari and Gandjalikhan Nassab [25] applied the blocked-off technique to study laminar forced convection of radiating gas over an inclined backward-facing step of a horizontal channel under bleeding condition. Bahraini et al. [26] used the conjugate gradient method in an inverse boundary design problem of combined radiation and convection to find the unknown power of heaters installed on the top wall a channel to perform uniform temperature and heat flux over the design surface. In that study, the discrete ordinate method (DOM) applied to solve the radiative transfer equation (RTE). The authors found that rising the step inclination angle increases the total heat flux over the heater surface. Recently, the interaction of mixed convection and surface radiation on thermally developing laminar flow in a horizontal with variable side-heated wall was studied by Rajamohan et al. [27].

In the previous research works mentioned in the field of the combined radiation and convection heat transfer, the boundary surfaces considered as diffuse-gray ones. In such boundaries, radiative properties such as emissivity are independent of wavelength and temperature, while in many practical situations, the surfaces treat as diffuse-spectral ones. Omidpanah et al. [28] estimated the unknown temperature distribution over the heater surface mounted on the upper wall of a two-dimensional rectangular duct to produce uniform heat flux and temperature distribution over the design surface. In that inverse boundary design problem, the researchers considered the design surface as a diffuse-spectral boundary that its emissivity is a function of wavelength and temperature, while the heater treated as diffuse-gray one. The conjugate gradient method applied to solve the inverse problem while the RTE solved via DOM. The results indicate that the heaters need more power when a diffuse-spectral surface is used instead of a diffuse-gray one.

Arendt et al. [29] numerically and analytically analyzed the static and dynamic thermal behaviors of hollow bricks considering various cavity concentrations. The obtained results depicted a non-linear relationship between the thermal conductivity and cavity concentration of the hollow bricks. Sun et al. [30] conducted a 3-D simulation of concrete hollow brick by the finite volume method (FVM). They studied 240×115×90 concrete hollow bricks with 71 configurations. As they reported, equivalent thermal conductivity (ETC) is a decreasing function of enclosure numbers in the parallel direction of heat transfer. Li et al. [31] conducted a numerical simulation of the

multi-holed clay brick with the dimension of 240×115×90 in 50 kinds of holes and arrangements. The results showed that radiation was a decreasing function of the hole numbers. They also found that equivalent thermal conductivity depended on thermal conductivity of the solid media.

Although a few studies have explored the combined natural convection and volumetric radiation in hollow bricks with conducting walls, the simulation of heat transfer through hollow bricks has not been investigated in the transient conditions. Therefore, the main objective of this research was to conduct a numerical investigation over the effects of geometry and wall emissivity on the thermal behavior with respect to time.

2. Analysis

Two-dimensional combined convection and radiation heat transfer in fluid flow and conduction heat transfer in a solid body of the hollow bricks were numerically simulated. Schematics of the computational domain and dimension are illustrated in Fig.1 and Table 1, respectively. The related governing equations can be written as follows.

The equations for transient combined conduction, convection, and radiation fluid and solid medium, known as conjugate heat transfer were non-dimensionalized by the following parameters, which can be expressed as follows:

$$U=\frac{uL}{\alpha_f}.V=\frac{vL}{\alpha_f}.X=\frac{x}{L}.Y=\frac{y}{L}$$

$$t^*=\frac{t}{\alpha_f L^2}.\theta=\frac{(T-T_c)}{\Delta T}.P=\frac{pL^2}{\rho\alpha_f^2}.\bar{I}=\frac{I}{\sigma T_c^4}$$

$$S=\frac{s}{L}.Q=\frac{q}{\sigma T_c^4}.Pr=\frac{\vartheta}{\alpha_f}.Ra=\frac{\beta G\Delta T L^3}{\vartheta\alpha_f}. \quad (1)$$

$$Pl=\frac{k_f}{L\sigma T_c^3}.\emptyset=\frac{\Delta T}{T_c}$$

Gas domain:

$$\frac{\partial U}{\partial X}+\frac{\partial U}{\partial Y}=0 \quad (2)$$

$$\frac{\partial U}{\partial t^*}+U\frac{\partial U}{\partial X}+V\frac{\partial U}{\partial Y}$$

$$=-\frac{\partial p}{\partial X}+\Pr\left(\frac{\partial^2 U}{\partial X^2}+\frac{\partial^2 U}{\partial Y^2}\right) \quad (3)$$

$$\frac{\partial V}{\partial t^*}+U\frac{\partial V}{\partial X}+V\frac{\partial V}{\partial Y}=-\frac{\partial p}{\partial Y}$$

$$+\Pr\left(\frac{\partial^2 V}{\partial X^2}+\frac{\partial^2 V}{\partial Y^2}\right)+RaPr(\theta-\theta_{ave}) \quad (4)$$

$$\frac{\partial\theta_f}{\partial t^*}+U\frac{\partial\theta_f}{\partial X}+V\frac{\partial\theta_f}{\partial Y}=$$

$$\left(\frac{\partial^2\theta_f}{\partial X^2}+\frac{\partial^2\theta_f}{\partial Y^2}\right)-\frac{1}{pL}\nabla^*.Q_r \quad (5)$$

Where in above equations, θ_{ave} is equal to zero. Solid domain:

$$\frac{\partial\theta_s}{\partial t^*}=\frac{\alpha_s}{\alpha_f}\left(\frac{\partial^2\theta_{Fs}}{\partial X^2}+\frac{\partial^2\theta_s}{\partial Y^2}\right) \quad (6)$$

In the aforementioned equations, the Boussinesq approximation was used in order to model the buoyancy effect. In the energy equation of gas medium, the term 'radiative' represented radiative flux divergence.

2.1. Gas Radiation Modeling

In an emitting, absorbing, and scattering medium the principal equations were stated by Modest [32]. The non-dimensional divergence of the radiation flux vector can be calculated as:

$$\nabla^*.Q_r=\tau(1-\omega)(4(\theta\emptyset+1)^4-\int_{4\pi}\bar{I}d\Omega) \quad (7)$$

In the above equation, $\bar{I}$ is the local intensity that can be obtained by radiative transport equation:

$$\frac{1}{\tau}(\Omega\nabla^*)\bar{I}=\frac{(1-\omega)}{\pi}(\theta\emptyset+1)^4-\bar{I}$$

$$+\frac{\omega}{4\pi}\int_{4\pi}\bar{I}\Phi d\acute{\Omega}) \quad (8)$$

Where, Φ is the scattering phase function. Its value was considered unity in this study since it represents an isotropic scattering medium.

2.2. Initial and Boundary Conditions

Initially, the velocity components were considered zero and the temperature field inside the hollow bricks was uniform and equal to the cold wall. Therefore, the non-dimensional initial conditions were as:

$$U(X.Y.0)=V(X.Y.0)=P(X.Y.0)$$

$$=\theta(X.Y.0)=0 \quad (9)$$

According to the non-slip condition in the interface boundaries, the velocity components at all times were written as:

$$U=V=0 \quad (10)$$

In terms of thermal boundary conditions, the right and left sides were considered cold and hot, respectively, and the top and bottom sides were isolated. So, the relation can be stated as:

$$\theta(0.Y.t^*)=1.\ \theta(1.Y.t^*)=0.$$

$$\frac{\partial\theta(X.0.t^*)}{\partial Y}=\frac{\partial\theta(X.1.t^*)}{\partial Y}=0 \quad (11)$$

Table 1. Dimensions of the hollow bricks

a=a'/(L+2a')=a'/L'	H=H'/(L+2a')=H'/L'	L =l'/(L+2a')=l'/L'
0.1	0.35	0.8

According to the continuity of heat flux principle at the interface boundary condition, the mentioned boundary condition can be written as:

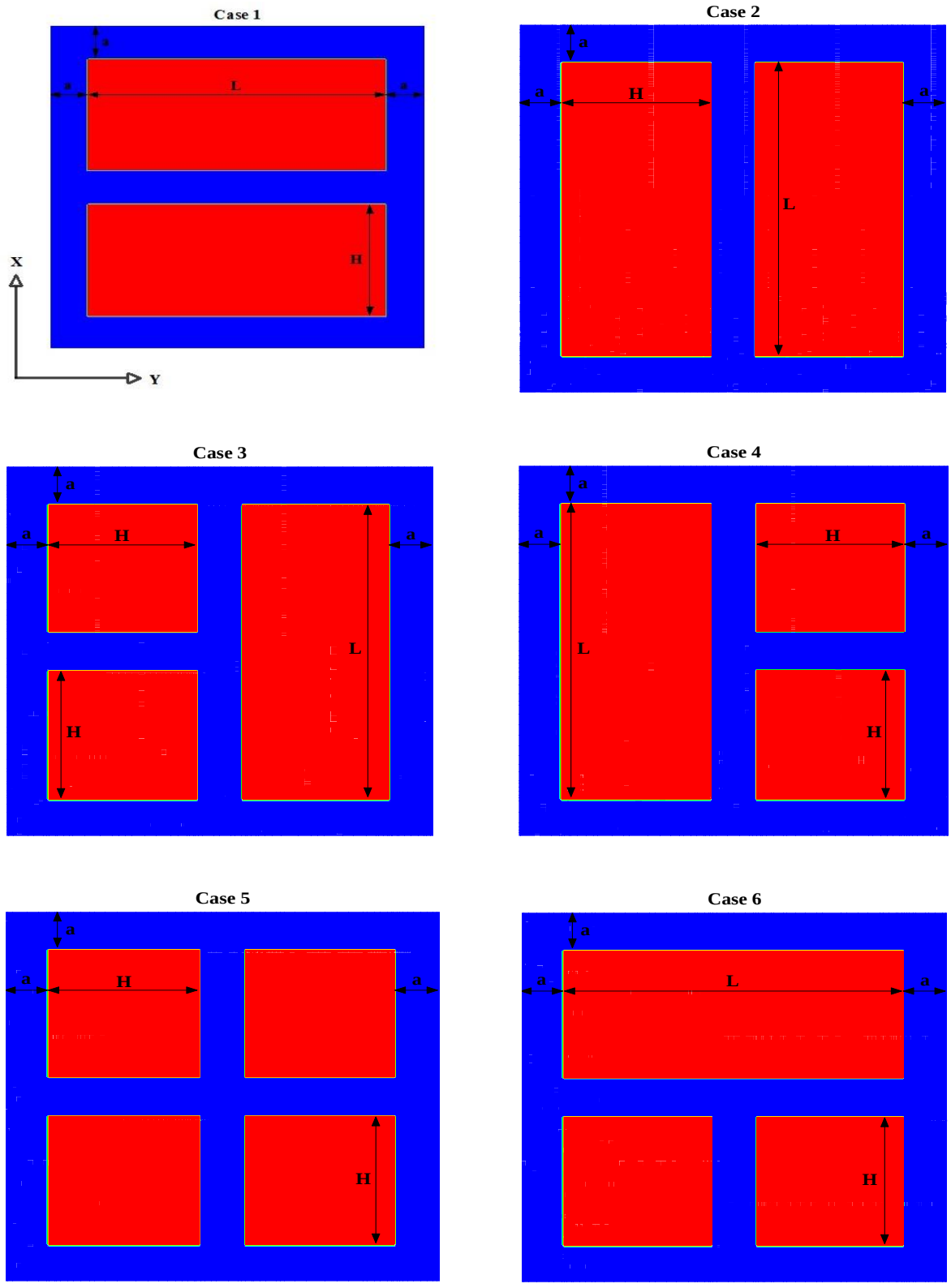

Figure 1. Schematics of the hollow bricks

$$\left[-K\frac{\partial\theta_s}{\partial n}\right]_s = \left[-\frac{\partial\theta_f}{\partial n}\right]_f + \frac{\tau\epsilon_w}{Pl\emptyset}$$

$$\left[4(\theta\emptyset+1)^4 - \sum_{ns_w} I^*(r_w, t^*)|r_w.s_w|\right] w_i \quad (12)$$

$$\theta_s = \theta_f$$

In this equation, K represents the ratio of solid to gas thermal conductivity and n is a unity normal vector to the interface boundary

The radiative boundary condition for a diffusing and reflecting interface boundary can be represented as:

$$I(r_w,\Omega) = \epsilon I_b(r_w) + \frac{(1-\varepsilon)}{\pi}\int_{n.\acute{\Omega}<0} I(r_w,\acute{\Omega})|n.\acute{\Omega}|\,d\acute{\Omega} \quad (13)$$

Furthermore, at any time step, the distribution of the overall heat flux and its average on the cold wall can be calculated as:

$$Q_{ave} = K\frac{\partial\theta}{\partial X}\Big|_{X=L} \quad (14)$$

$$\overline{Q_{ave}} = \int K\frac{\partial\theta}{\partial X}\Big|_{X=L} dY \quad (15)$$

3. Numerical Procedure

To accurately solve the governing equations in solid and fluid media, FVM was applied. To estimate the non-linear terms in energy equation of fluid region and interface boundary equation, the alternating direction implicit method was used. According to this method, the mentioned relationship can be written as:

$$\left(\frac{\partial\theta_f}{\partial t^*}\right) + \left(U\frac{\partial v}{\partial X}\right)_{m+1} + \left(V\frac{\partial v}{\partial Y}\right)_m = \left(\frac{\partial^2\theta_f}{\partial X^2}\right)_{m+1} + \left(\frac{\partial^2\theta_f}{\partial Y^2}\right)_m - \frac{\tau(1-\omega)}{Pl\emptyset} \quad (16)$$

$$\left[4\left(\theta_f\emptyset+1\right)^4 - \sum_{i=1}^{n} I_i^* w_i\right]_m$$

$$\left(\frac{\partial\theta_f}{\partial t^*}\right) + \left(U\frac{\partial\theta_f}{\partial X}\right)_{m+1} + \left(V\frac{\partial\theta_f}{\partial Y}\right)_{m+2} = \left(\frac{\partial^2\theta_f}{\partial X^2}\right)_{m+1} + \left(\frac{\partial^2\theta_f}{\partial Y^2}\right)_{m+2} - \frac{\tau(1-\omega)}{Pl\emptyset} \quad (17)$$

$$\left[4\left(\theta_f\emptyset+1\right)^4 - \sum_{i=1}^{n} I_i^* w_i\right]_{m+1}$$

$$\left(\frac{\partial\theta_s}{\partial t^*}\right) = \frac{\alpha_s}{\alpha_f}\left(\left(\frac{\partial^2\theta_s}{\partial X^2}\right)_{m+1} + \left(\frac{\partial^2\theta_s}{\partial Y^2}\right)_m\right) \quad (18)$$

$$\left(\frac{\partial\theta_s}{\partial t^*}\right) = \frac{\alpha_s}{\alpha_f}\left(\left(\frac{\partial^2\theta_s}{\partial X^2}\right)_{m+1} + \left(\frac{\partial^2\theta_s}{\partial Y^2}\right)_{m+2}\right) \quad (19)$$

$$\left(\left[-K\frac{\partial\theta_s}{\partial n}\right]_s\right)_{m+1} = \left(\left[-\frac{\partial\theta_f}{\partial n}\right]_f\right)_{m+1} + \frac{\tau\epsilon_w}{Pl\emptyset}$$

$$\left[4(\theta\emptyset+1)^4 - \sum_{ns_w} I^*(r_w, t^*)|r_w.s_w|w_i\right]_m \quad (20)$$

where, m is the time step.

The applied numerical steps were below:

1- The unknown variables were initialized in time step Δt.
2- The components of velocity and temperature were simultaneously calculated by considering the relative source term.
3- RTE was solved by the obtained results, velocity, and temperature to update the radiative source term. Steps 2 and 3 were repeated until all equations converged in the current time step.
4- Steps 1-4 were repeated until all variables achieved steady-state conditions

To perform the above-mentioned steps, the equations were discretized concerning the mentioned techniques and written in Fortran, a well-known computer program. Moreover, for identifying the regions of each case, the blocked off method was applied. The details of this method were elaborately described in a previous study [4].

In each time step, the convergence criterion is as below:

$$Max\left|\frac{\emptyset_p^n - \emptyset_p^{n+1}}{\emptyset_p^n}\right| \le 10^{-6} \quad (21)$$

where, $\emptyset$ can be, $U.V.\theta$ and I_p

4. Grid refinement test

To find the best grid in terms of independence and time in each time step, numerous tests were conducted. The average overall heat transfer across the cold wall with different grid sizes is tabulated in Table 2. According to the findings, the grid sizes shown in row 3 are considered the optimum grid size for each case in this study. Note that the time interval of $\Delta t = 10^{-6}$ was used based on similar tests. In the computational domain, non-uniform grid was applied to reduce the computational time. Fig. 2 shows a schematic of the generated mesh for case 3, 4, 5 and 6

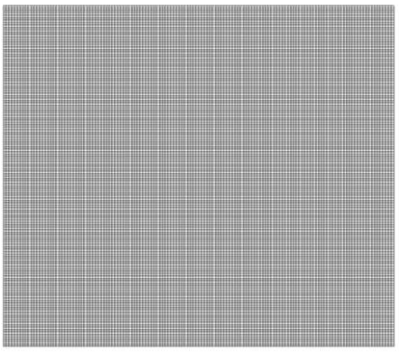

Figure 2. Sketch of the generated mesh (Case 3, 4, 5 and 6)

Table 2. The grid size effect

Case 1		Case 2		Case 3		Case 4		Case 5		Case 6	
Grid	$\overline{Q_{ave}}$	Grid	$\overline{Q_{ave}}$	Grid	$\overline{Q_{ave}}$	Grid	$\overline{Q_{ave}}$	Grid	$\overline{Q_{ave}}$	Grid	$\overline{Q_{ave}}$
90 ×60	29.297	60 ×100	23.856	80 × 80	24.557	80 × 80	23.044	80 × 80	27.001	80 × 80	28.654
120 × 80	32.258	80 × 120	25.001	120 × 120	27.036	120 × 120	27.965	120 × 120	31.045	120 × 120	31.002
140 × 100	35.313	100 ×140	26.305	140 ×140	28.425	140 ×140	29.096	140 ×140	32.456	140 ×140	32.294
160 × 120	35.808	120 × 160	26.909	160 × 160	29.001	160 × 160	29.856	160 × 160	32.987	160 × 160	32.902

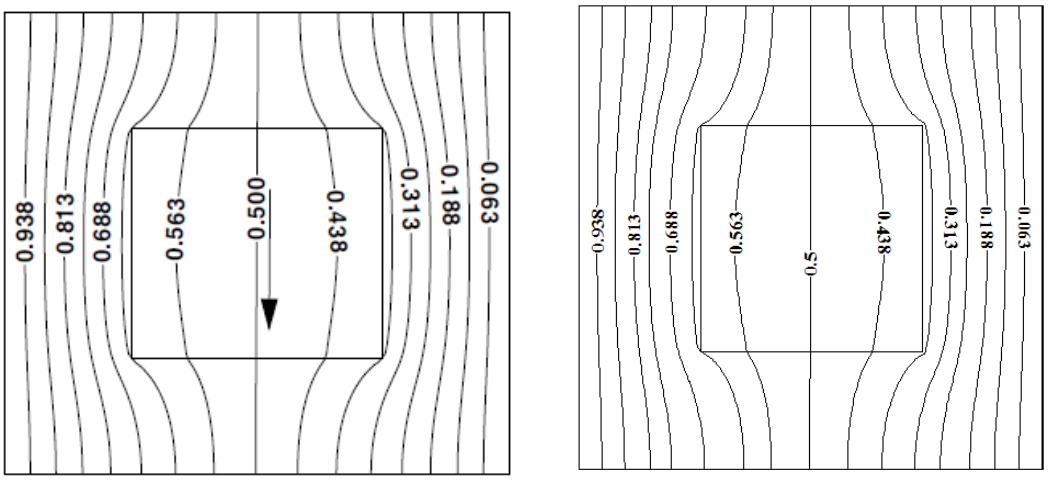

(a) Present study (b) Manab Kumar Das et al. [33]

Figure 3. The distribution of temperature in a cavity containing a conducting square block at Ra=10^3 and k_s/k_f= 5.

5. Validation

5.1. conjugate pure natural convection

To examine the numerical method used for conjugation of the natural convection, it was compared with the calculations provided by Manab Kumar Das et al. [33]. Figs. 3(a) and 3(b) show the distribution of temperature in the solid and fluid media, respectively. The computations were performed for a square cavity containing a conducting block. A comparison of these two figures indicates an excellent agreement between them.

5.2. combined natural conduction, convection and radiation

To check performance and accuracy of numerical techniques concerning the combined convection and volumetric radiation, a comparison was conducted between the numerical techniques used in the current study and those performed in a study by Byun and Hyukim [34]. All boundary walls were at isotherm condition, so that when a bottom was hot, the other boundaries were considered cold. Fig. 4 and Fig. 5 depict the streamlines and isotherm contours inside the enclosure, respectively. It is evident that an excellent agreement was obtained between them.

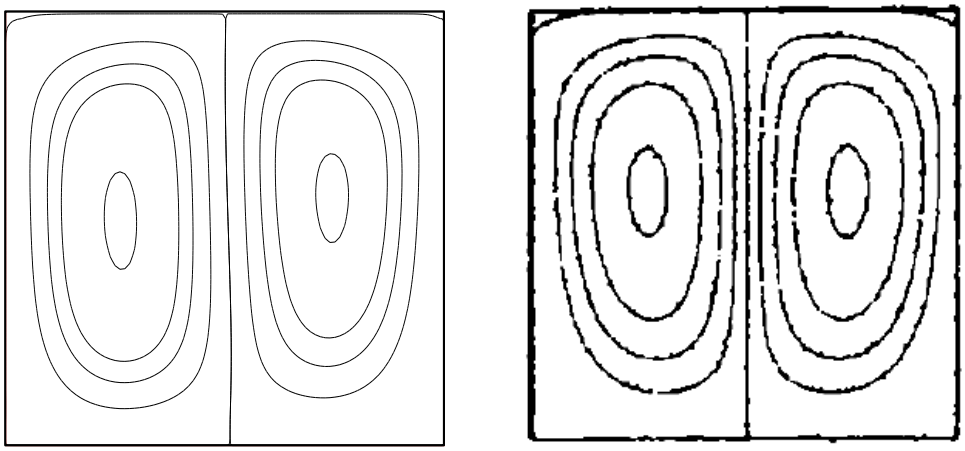

(a) Present study (b) Byun and Hyukim [34]

Figure 4. Distribution of the streamlines Ra = 0.92 × 106, *Pr* = 0.71, τ = 1, **ω** = 0.

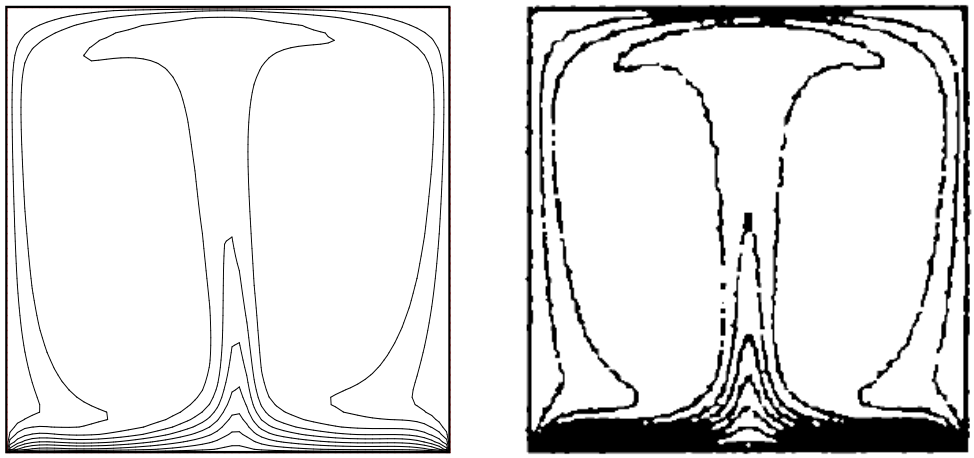

(a) Present study (b) Byun and Hyukim [34]

Figure 5. Distribution of the isotherm contours Ra = 0.92 × 106, *Pr* = 0.71, τ = 1, **ω** = 0.

6. Results and discussion

To simulate hollow bricks in terms of thermal and hydrodynamic performance, the standard-room conditions were considered. In this study, the fluid flow is assumed to be laminar, due to small dimensions of the problem and closed boundaries of bricks in a wall. Also, there is not any external flow or a tremendous heat source to increase the velocity in the hollow bricks. The calculated non-dimensional parameters are indicated in Table 3 [4].

To discuss the thermal and hydrodynamic behaviors of the investigated cases, Fig. 6 and Fig. 7 depicts the isotherms and streamlines of each case in the steady state condition, respectively. The graphs reveal that the geometry has significant and marginal effects on the velocity and temperature fields, respectively. In other words, in geometries with vertical rectangle sub cavities (cases 2, 3, and 4), the velocity is greater than other cases. Moreover, cases 3 and 4 can be considered identical in terms of maximum velocity. This phenomenon can be explained as the following reasons.

1- With regard to the gravity of the shape of sub cavities, the flow field can rotate with higher speeds and gas can gain more heat
2- In cases 3 and 4, the temperature difference is greater than case 2, as it is shown in Figs. 6 & 7.

Regarding the hollow bricks, horizontal rectangle and square sub cavities are concerned, since the temperature difference in sub cavities with horizontal rectangle shape is much greater than the square one and the intensity of flow is much bigger. For example, in case 6, the maximum value of the stream function is about -1.8 in the horizontal rectangles, and about -2.8 in the square one.

Table 1. Values of non-dimensional parameters

Parameter	Pl	Ra	Pr	K	α_s/α_f	ω	ε	φ
Value	0.15	10^6	0.71	75	4.3	0.5	0.9	0.06

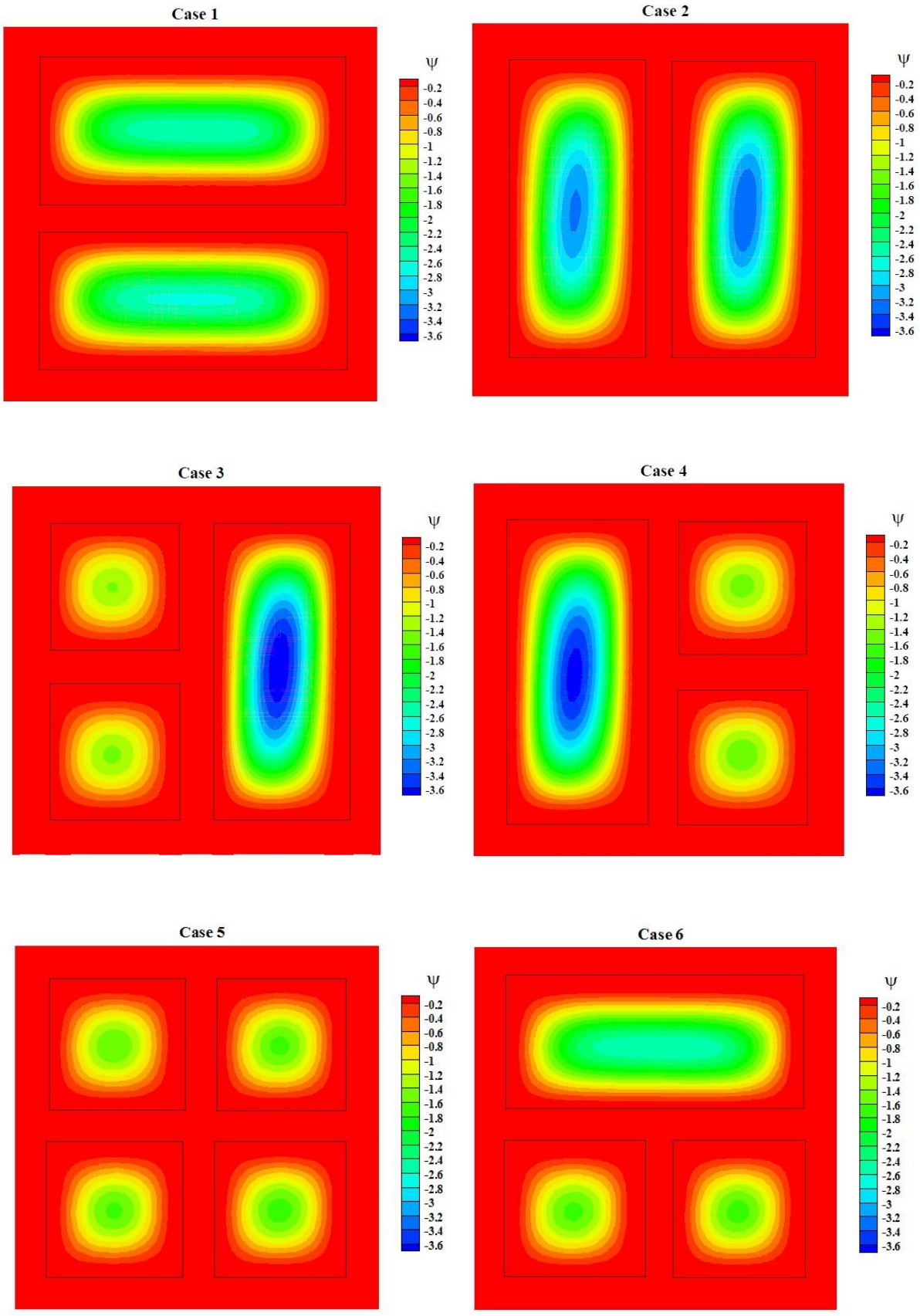

Figure 6. Contours of streamline

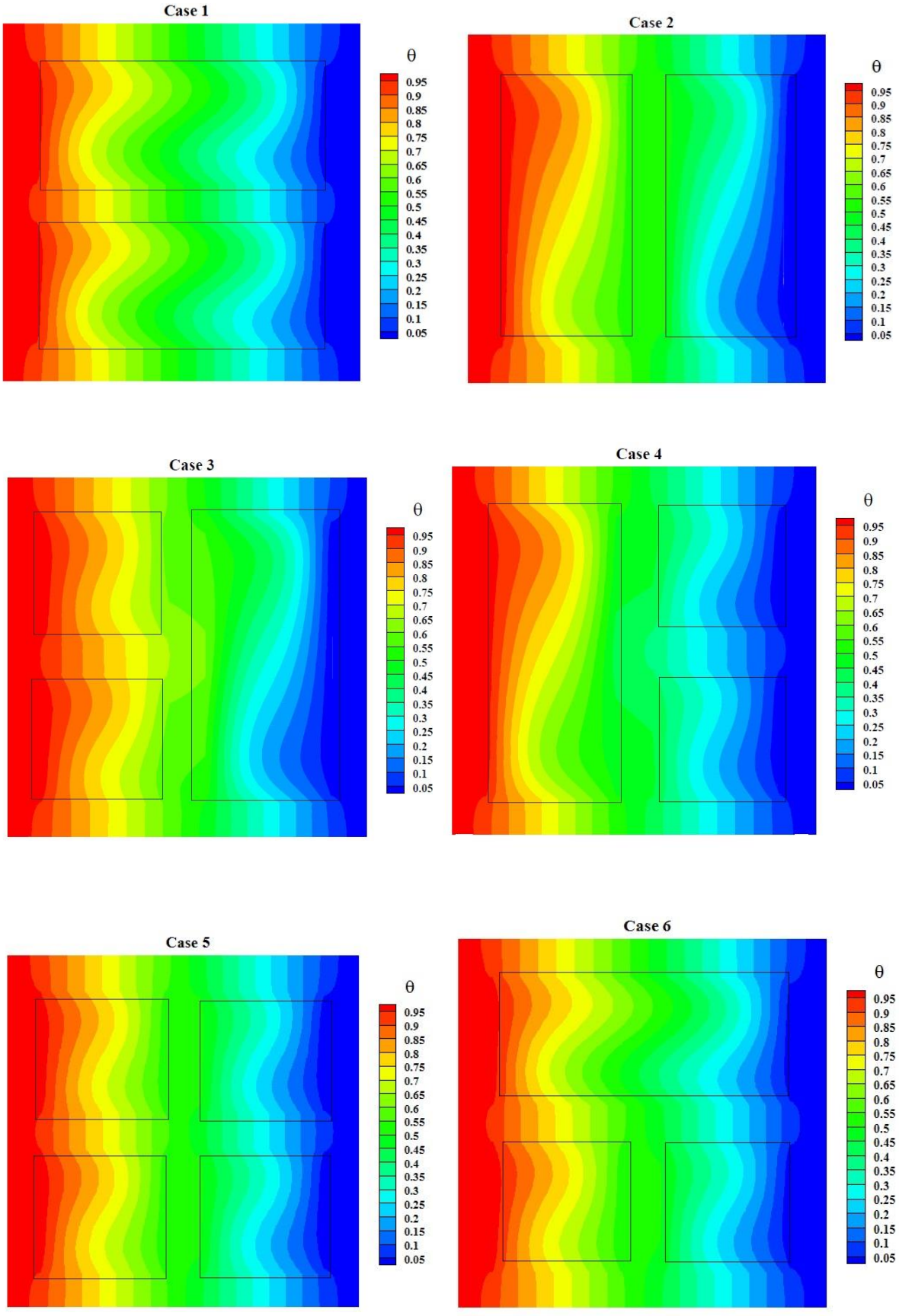

Figure 7. Contours of isotherm line

Fig. 8 represents the distribution of total heat flux through the cold wall in the steady state condition. Based on the provided data, 2 of 6 cases had different shapes, which were our favorite cases. In other words, in cases 2 and 3 the amount of heat flux is by far less than other cases. This is caused by detrimental effects of the mid horizontal wall connecting the mid of hollow bricks to the cold wall and the square shape of sub cavities located at the right side.

Fig. 9 depicts the average total heat flux of the cold wall concerning time for the study cases. So, by decreasing the amount of heat flux, the time of reaching the steady state condition increases moderately. Furthermore, cases 1 and 2 had the maximum and minimum values, respectively, which was due to the distribution of the total heat flux on the cold wall in the steady state condition (Fig. 8). Considering Fig. 8, it is evident that cases 1 and 2 have different shapes compared to other cases; in this regard the mid horizontal wall connecting the mid of hollow bricks to the cold wall and small cavities located at the right side can have damaging effects. It can be seen that the middle walls are the easiest way for heat transfer from one side to other side, while the flow rate is minimum in small cavities.

As mentioned before, the effect of radiative heat flux on these cases is paramount; so, an attempt was made to investigate the impact of emissivity coefficient. Furthermore, since it is feasible for manufacturers to cover the inside of bricks with materials with different emissivity coefficients, the results of this study are highly applicable. Fig. 10 demonstrates the average cold wall heat flux concerning time for various emissivity coefficients. The data revealed that the average heat flux was a decreasing function of emissivity coefficient. Furthermore, the time required to reach the steady state condition was an increasing function of emissivity coefficient.

Fig. 11 illustrates the distribution of total heat flux on the cold wall in steady-state conditions for various emissivity coefficients. According to this figure, the curves are not symmetric concerning the x-axis because natural convection causes the amount of heat flux to cross from the upper side of cold wall. The amount of heat transfer at y (0) was about 60, while the equivalent data in y (1) were 65.

Conclusion

Simulation of the combined mode of radiation and natural convection heat transfer through hollow bricks in transient conditions is studied in this work. The DOM used to solve the radiative transfer equation and block off method applied to distinguish between solid and fluid media in the computational domain. The findings showed that the vertical rectangle sub cavities in hollow bricks, especially those located at the cold wall had beneficial effects on the performance of hollow bricks in terms of heat transfer. The time required to reach the steady state condition was a decreasing function of the average total heat flux. The impact of radiation heat transfer on the cases under study was remarkable so that the amount of heat flux was a decreasing function of emissivity coefficient

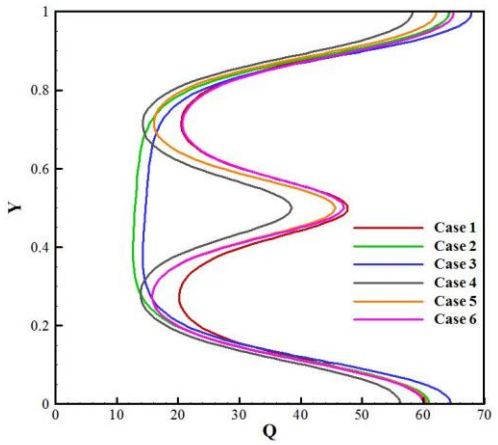

Figure 8. Distribution of total heat flux on cold wall in steady state for various cases

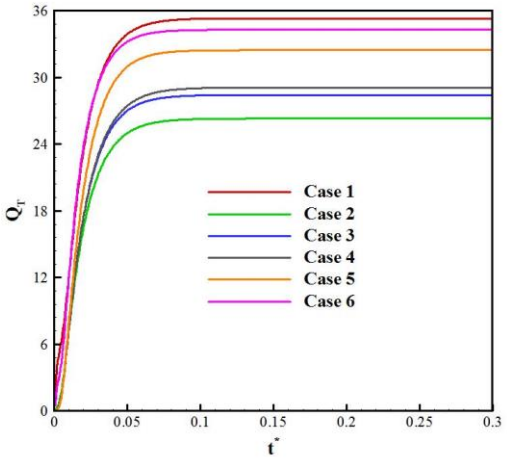

Figure 9. Total heat flux on cold wall concerning time for various cases

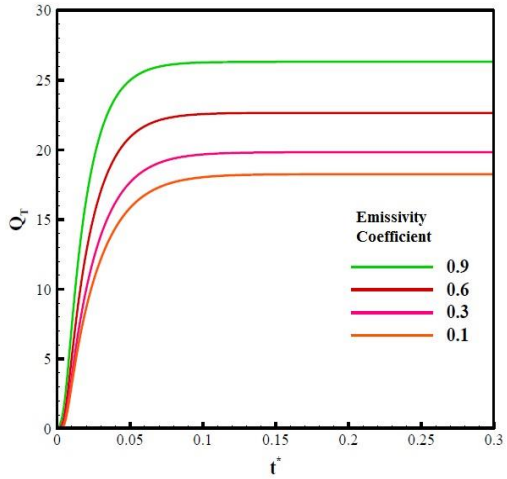

Figure 10. Total heat flux on cold wall concerning time for various emissivity confection in case 2

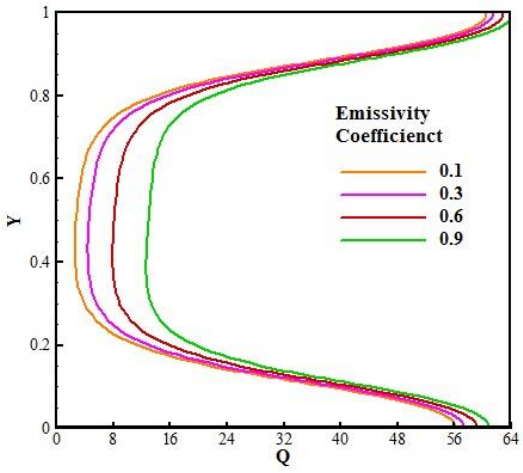

Figure 11. Distribution of the total heat flux on cold wall in steady state for various emissivity confection in case 2

Nomenclature

u,v	Velocity components (dimensional)
β	Volume expansion coefficient
p	Pressure (dimensional)
ρ	Density
g	Gravity acceleration
ϑ	Kinematic viscosity
T	Temperature (dimensional)
K	Thermal conductivity
P	Pressure (dimensionless)
I	Local intensity
t	Time
Pr	Prandtl number
X,Y	Horizontal and vertical coordinates (dimensionless)
U,V	Velocity components (dimensionless)
L	Length
n	Unity vector
Φ	Scattering phase function
Ra	Rayleigh number
τ	Optical thickness
ω	Weighting factor

References

[1] Moufekkir, F., M. A. Moussaoui, A. Mezrhab, H. Naji, and D. Lemonnier. "Numerical prediction of heat transfer by natural convection and radiation in an enclosure filled with an isotropic scattering medium." Journal of Quantitative Spectroscopy and Radiative Transfer 113, no. 13 (2012): 1689-1704.

[2] Vivek, V., Anil Kumar Sharma, and C. Balaji. "Interaction effects between laminar natural convection and surface radiation in tilted square and shallow enclosures." International Journal of Thermal Sciences 60 (2012): 70-84.

[3] Zhang, Wei, Chuhua Zhang, and Guang Xi. "Conjugate conduction-natural convection in an enclosure with time-periodic sidewall temperature and inclination." International Journal of Heat and Fluid Flow 32, no. 1 (2011): 52-64.

[4] Nia, Mohammad Foruzan, Seyyed Abdolreza Gandjalikhan Nassab, and Amir Babak Ansari. "Transient combined natural convection and radiation in a double space cavity with conducting walls." International Journal of Thermal Sciences 128 (2018): 94-104.

[5] Martyushev, Semen G., and Mikhail A. Sheremet. "Conjugate natural convection combined with surface thermal radiation in a three-dimensional enclosure with a heat source." International Journal of Heat and Mass Transfer 73 (2014): 340-353.

[6] Al-Hazmy, Majed M. "Analysis of coupled natural convection–conduction effects on the heat transport through hollow building blocks." Energy and Buildings 38, no. 5 (2006): 515-521.

[7] Young, T. J., & Vafai, K. (1998). Convective flow and heat transfer in a channel containing multiple heated obstacles. International Journal of Heat and Mass Transfer, 41(21), 3279-3298.

[8] Kim, S. Y., Kang, B. H., & Jaluria, Y. (1998). Thermal interaction between isolated heated electronic components in pulsating channel flow. Numerical Heat Transfer, Part A Applications, 34(1), 1-21.

[9] Bhowmik, H., Tso, C. P., Tou, K. W., & Tan, F. L. (2005). Convection heat transfer from discrete heat sources in a liquid cooled rectangular channel. Applied Thermal Engineering, 25(16), 2532-2542.

[10] Hamouche, A., & Bessaïh, R. (2009). Mixed convection air cooling of protruding heat sources mounted in a horizontal channel. International Communications in Heat and Mass Transfer, 36(8), 841-849.

[11] Yang, M. H., Yeh, R. H., & Hwang, J. J. (2010). Mixed convective cooling of a fin in a channel. International Journal of Heat and Mass Transfer, 53(4), 760-771.

[12] Boutina, L., & Bessaïh, R. (2011). Numerical simulation of mixed convection air-cooling of electronic components mounted in an inclined channel. Applied Thermal Engineering, 31(11-12), 2052-2062.

[13] Mathews, R. N., & Balaji, C. (2006). Numerical simulation of conjugate, turbulent mixed convection heat transfer in a vertical channel with discrete heat sources. International

communications in heat and mass transfer, 33(7), 908-916.
[14] Premachandran, B., & Balaji, C. (2006). Conjugate mixed convection with surface radiation from a horizontal channel with protruding heat sources. International Journal of Heat and Mass Transfer, 49(19-20), 3568-3582.
[15] Pirouz, M. M., Farhadi, M., Sedighi, K., Nemati, H., & Fattahi, E. (2011). Lattice Boltzmann simulation of conjugate heat transfer in a rectangular channel with wall-mounted obstacles. Scientia Iranica, 18(2), 213-221.
[16] Kheirandish, Z., Nassab, S. G., & Vakilian, M. (2013). Second law analysis of forced convective cooling in a channel with a heated wall mounted obstacle. Journal of Electronics Cooling and Thermal Control, 3(03), 101.
[17] Datta, A., Sharma, V., Sanyal, D., & Das, P. (2019). A conjugate heat transfer analysis of performance for rectangular microchannel with trapezoidal cavities and ribs. International Journal of Thermal Sciences, 138, 425-446.
[18] Bilir, Ş., & Ateş, A. (2003). Transient conjugated heat transfer in thick walled pipes with convective boundary conditions. International Journal of Heat and Mass Transfer, 46(14), 2701-2709.
[19] Perng, S. W., & Wu, H. W. (2008). Numerical investigation of mixed convective heat transfer for unsteady turbulent flow over heated blocks in a horizontal channel. International Journal of Thermal Sciences, 47(5), 620-632.
[20] Knupp, D. C., Cotta, R. M., Naveira-Cotta, C. P., & Kakaç, S. (2015). Transient conjugated heat transfer in microchannels: integral transforms with single domain formulation. International Journal of Thermal Sciences, 88, 248-257.
[21] Viskanta, R. (1998). Overview of convection and radiation in high temperature gas flows. International Journal of Engineering Science, 36(12-14), 1677-1699.
[22] Azad, F. H., & Modest, M. F. (1981). Combined radiation and convection in absorbing, emitting and anisotropically scattering gas-particulate tube flow. International Journal of Heat and Mass Transfer, 24(10), 1681-1698.
[23] Chiu, H. C., & Yan, W. M. (2008). Mixed convection heat transfer in inclined rectangular ducts with radiation effects. International Journal of Heat and Mass Transfer, 51(5-6), 1085-1094.
[24] Barhaghi, D. G., & Davidson, L. (2009). Large-eddy simulation of mixed convection-radiation heat transfer in a vertical channel. International Journal of Heat and Mass Transfer, 52(17-18), 3918-3928.
[25] Ansari, A. B., & Nassab, S. G. (2011). Study of laminar forced convection of radiating gas over an inclined backward facing step under bleeding condition using the blocked-off method. Journal of heat transfer, 133(7), 072702.
[26] Bahraini, S., Nassab, S. G., & Sarvari, S. M. H. (2016). Inverse Convection–Radiation Boundary Design Problem of Recess Flow with Different Conditions. Iranian Journal of Science and Technology, Transactions of Mechanical Engineering, 40(3), 215-222.
[27] Rajamohan, G., Ramesh, N., & Kumar, P. (2019). Mixed convection and radiation studies on thermally developing laminar flow in a horizontal square channel with variable side heated wall. International Journal of Thermal Sciences, 140, 298-307.
[28] Omidpanah, M., & Gandjalikhan Nassab, S. A. (2019). Inverse Boundary Design Problem of Combined Radiation Convection Heat Transfer in a Duct with Diffuse-Spectral Design Surface. Thermal Science, 23(1).
[29] Arendt, Krzysztof, Marek Krzaczek, and Jarosław Florczuk. "Numerical analysis by FEM and analytical study of the dynamic thermal behavior of hollow bricks with different cavity concentration." International Journal of Thermal Sciences 50, no. 8 (2011): 1543-1553.
[30] Sun, Jiapeng, and Liang Fang. "Numerical simulation of concrete hollow bricks by the finite volume method." International Journal of Heat and Mass Transfer 52, no. 23-24 (2009): 5598-5607.
[31] Li, L. P., Z. G. Wu, Z. Y. Li, Y. L. He, and W. Q. Tao. "Numerical thermal optimization of the configuration of multi-holed clay bricks used for constructing building walls by the finite volume method." International Journal of Heat and Mass Transfer 51, no. 13-14 (2008): 3669-3682.
[32] M. Modest, Radiative heat transfer, Academic Press, 2013
[33] Das, Manab Kumar, and K. Saran Kumar Reddy. (2006). Conjugate natural convection heat transfer in an inclined square cavity containing a conducting block. International Journal of Heat and Mass Transfer 49.25-26: 4987-5000.
[34] Byun, Ki-Hong; IM, Moon Hyuk. (2002). Radiation-laminar free convection in a square duct with specular reflection by absorbing-emitting medium. KSME international journal 16.10: 1346-1354.